

Choptuik scaling in null coordinates

David Garfinkle

Dept. of Physics, Oakland University, Rochester, MI 48309

email: garfinkl@vela.acs.oakland.edu

Abstract

A numerical simulation is performed of the gravitational collapse of a spherically symmetric scalar field. The algorithm uses the null initial value formulation of the Einstein-scalar equations, but does *not* use adaptive mesh refinement. A study is made of the critical phenomena found by Choptuik in this system. In particular it is verified that the critical solution exhibits periodic self-similarity. This work thus provides a simple algorithm that gives verification of the Choptuik results.

arXiv:gr-qc/9412008v1 2 Dec 1994

I. INTRODUCTION

Recently Choptuik has discovered scaling behavior in the collapse of a spherically symmetric scalar field to form a black hole. [1] Choptuik numerically evolves a family of initial data parametrized by p to find that the mass of the black hole is $M \propto (p - p^*)^\gamma$ where p^* is the critical value of p and γ is the scaling exponent. For the data with $p = p^*$, a zero mass singularity forms. This critical solution has the property of periodic self-similarity: the scalar field evolves, after a certain amount of time, to a copy of its profile with the scale of space shrunk. Similar results have been found by Abrahams and Evans [2] for vacuum axisymmetric gravitational collapse.

To treat the critical solution the parameter p must be tuned to p^* to great accuracy. In addition the size of features must be resolved on extremely small scales. Therefore one might worry that the periodic self-similarity of the critical solution could be an artifact of the numerical algorithms used rather than the actual behavior of the collapse of a scalar field. The most straightforward way to show that the results of [1] are not numerical artifacts is to perform a numerical treatment of the same physical problem using a completely different algorithm. However, any accurate treatment of the critical solution must be able to resolve features on extremely small scales. Choptuik achieved this by using an adaptive mesh refinement algorithm. Since adaptive mesh refinement algorithms are fairly complicated it is not a trivial task to produce another adaptive mesh refinement code to redo the Choptuik result. Even with such a code one might worry that the results are an artifact of adaptive mesh refinement. In this paper I present results of a numerical simulation of the critical collapse of a scalar field. The algorithm uses the null initial value formulation of the problem, rather than the spacelike initial value formulation used in [1]. In addition, no adaptive mesh refinement is used. I find results in agreement with those of Choptuik. Section II describes the null initial formulation of the collapse of a spherically symmetric scalar field. Section III is a description of the numerical algorithm used to evolve this system. Section IV contains the results.

II. NULL INITIAL VALUE FORMULATION

The null initial value formulation for the collapse of a spherically symmetric scalar field was worked out by Christodoulou. [3] In this section we review this formulation and introduce the notation to be used in the rest of the paper. The Einstein-scalar equations are

$$R_{ab} = 8\pi \nabla_a \Phi \nabla_b \Phi \quad (1)$$

where R_{ab} is the Ricci tensor and Φ is the scalar field.

Null coordinates u and v are defined as follows: u is the proper time of an observer at the origin and is constant on outgoing light rays; $u = 0$ is the initial data surface. The coordinate v is constant on ingoing light rays and is equal to the usual area coordinate r on the initial data surface. (In what follows r will be regarded as a function of u and v).

For any quantity f define \dot{f} , f' and \bar{f} by

$$\dot{f} \equiv \frac{\partial f}{\partial u} \quad , \quad (2)$$

$$f' \equiv \frac{\partial f}{\partial v} \quad , \quad (3)$$

$$\bar{f} \equiv \frac{1}{r} \int_0^v f(u, \tilde{v}) r'(u, \tilde{v}) d\tilde{v} \quad . \quad (4)$$

Let h be the scalar such that $\bar{h} = \Phi$. Then as a consequence of Einstein's equations the metric can be written in terms of h and r . Define the quantities q and g by

$$q \equiv r^{-1} (h - \bar{h})^2 \quad , \quad (5)$$

$$g \equiv \exp(4\pi r \bar{q}) \quad . \quad (6)$$

Then the metric is

$$ds^2 = -2 g r' du dv + r^2 d\Omega^2 \quad . \quad (7)$$

Here $d\Omega^2$ is the two-sphere metric. Einstein's equations also provide evolution equations for h and r . These are [3]

$$\dot{h} = \frac{1}{2r} (g - \bar{g}) (h - \bar{h}) \quad , \quad (8)$$

$$\dot{r} = -\frac{1}{2} \bar{g} \quad . \quad (9)$$

III. NUMERICAL METHODS

A numerical simulation of these equations was first performed by Goldwirth and Piran. [4] A version of this algorithm was applied to the Choptuik problem by Grundlach, Price and Pullin. [5] However, the methods of references [4,5] are not accurate enough to treat the critical solution. I will start by discussing those features that my algorithm has in common with these earlier treatments and then present the new features that give the improvements in accuracy.

Initial data for the Einstein-scalar equations is just the value of h on the initial data surface. One evolves these equations as follows: [4,5] first one finds in succession the quantities \bar{h} , q , g and \bar{g} . This is done by evaluating the integrals for these quantities using Simpson's rule for unequally spaced points. Then the equations for \dot{h} and \dot{r} are used to evolve h and r forward one time step. This process is iterated as many times as necessary: *i.e.* until either a black hole forms or the field disperses. To find whether a black hole forms one looks for a marginally outer trapped surface. For spherical symmetry this is a surface for which $\nabla^a r \nabla_a r = 0$. (In practice the code cannot evolve up to the marginally outer trapped surface so one looks for the condition $\nabla^a r \nabla_a r \rightarrow 0$.) Since such a surface has $r = 2M$ the mass of the black hole is then half the radius of the marginally outer trapped surface.

In [5] this method was used to study the scaling behavior of the mass of the black hole. However, the method is not accurate enough for a treatment of the critical solution. I will now describe the sources of inaccuracy and the methods that my code uses to overcome

them. One source of inaccuracy comes from the fact that one divides by r in evaluating the quantities \bar{h} , q and \bar{g} . This leads to inaccuracies near $r = 0$. The second source of inaccuracy comes from the behavior of the critical solution. As the critical solution evolves its structure appears on ever smaller spatial scales. With a fixed spatial resolution there comes a time when the number of grid points is not sufficient to resolve the structure of the scalar field.

My code overcomes the first source of inaccuracy as follows: first expand h in a Taylor series in r .

$$h = h_0 + h_1 r + O(r^2) \quad , \quad (10)$$

Then the Taylor series for \bar{h} , q , g and \bar{g} are given by

$$\bar{h} = h_0 + \frac{1}{2} h_1 r + O(r^2) \quad , \quad (11)$$

$$q = \frac{1}{4} h_1^2 r + O(r^2) \quad , \quad (12)$$

$$g = 1 + \frac{\pi}{2} h_1^2 r + O(r^2) \quad . \quad (13)$$

$$\bar{g} = 1 + \frac{\pi}{4} h_1^2 r + O(r^2) \quad . \quad (14)$$

Thus to find the behavior of all quantities near the origin one needs to find only h_0 and h_1 . This is done by fitting the first four values of h to a line. Equations (11-14) are then used to find the values of \bar{h} , q , g and \bar{g} for the first three values of r . The Simpson's rule integration is then used for all other values of r .

The inaccuracy due to poor spatial resolution is solved as follows: first note that the inaccuracy is due to the size of the spatial structure being much smaller than the overall size of the grid. However, in the null initial value formulation the grid points are tied to ingoing light rays. Thus as the system evolves the overall size of the grid becomes smaller and the resolution improves. The critical solution forms a zero mass singularity. Consider the ingoing light ray that just barely hits this singularity. Choose the outermost gridpoint

to correspond to this light ray. Then the size of the grid shrinks as much as the size of the spatial features and thus the resolution is always good. In practice one does not know beforehand the position on the initial data surface of the light ray that just barely hits the singularity. Therefore I have run the code as follows: First I make an estimate of where the outermost gridpoint should be and choose the point to be slightly higher than the estimate. This ensures that the evolution will proceed for a while with good resolution. However, after a certain amount of time, because the outermost grid point is too far, the spatial features will come to occupy a relatively small number of grid points. Observation of the size of the spatial features at this time allows a refined estimate for the position of the outermost grid point. This refined estimate is then used to choose a (slightly too large) outermost gridpoint. This whole process is then iterated (a few times) until the outermost gridpoint corresponds, with good accuracy to the light ray that just barely hits the singularity.

In this way the overall size of the grid shrinks in proportion to the size of the spatial features. However, it is still the case that the number of grid points decreases during the evolution. This is because each grid point corresponds to an ingoing light ray. The grid point is therefore lost when the light ray hits the origin. This difficulty is dealt with in the code as follows: the evolution proceeds until half of the grid points are lost. These grid points are then interpolated halfway in between each of the remaining grid points. Thus over time the number of gridpoints is maintained.

This algorithm is far simpler (though far more specialized) than adaptive mesh refinement. The code was about 200 lines of Fortran.

Although this algorithm is well suited for a study of the critical solution, it is not so well suited for a study of the scaling behavior of the mass of the black hole. In treating the critical solution a great deal of accuracy was gained by choosing the outermost gridpoint to be the null geodesic that just barely hits the singularity. However, in treating the formation of a black hole the outermost gridpoint must be chosen sufficiently far that the corresponding geodesic does not hit the origin before the formation of a marginally outer trapped surface. When treating a range of p the outermost gridpoint must satisfy this condition for every

spacetime in the one parameter family. But then for p sufficiently close to p^* the spatial resolution will not be good enough to resolve the spatial structure of the solution. Therefore only a limited range of p can be treated using this algorithm.

IV. RESULTS

All runs were done with 300 spatial gridpoints. The code was developed and run on a NeXT workstation. Then for higher accuracy it was run on a Cray Y-MP. The initial data for the scalar field Φ on the $u = 0$ surface was

$$\Phi(r) = \phi_0 r^2 \exp \left[- \left(\frac{r - r_0}{\sigma} \right)^2 \right] \quad (15)$$

where ϕ_0 , r_0 and σ are constants. Thus the initial value of Φ has essentially a gaussian profile of width σ centered about a spherical shell of radius r_0 . The values of σ and r_0 are fixed, while the amplitude ϕ_0 is the parameter p .

The code was first run to find the critical value of the parameter p . This was done by a binary search: a parameter that led to the formation of a black hole was higher than the critical parameter. One that did not lead to black hole formation was smaller than the critical value. The next estimate of the critical parameter was chosen halfway between one known to be too high and one known to be too low. This process was iterated until the critical value of the parameter was found to the needed accuracy. At the same time the value of the outermost gridpoint was chosen as described in the previous section.

The code was then run to examine the scaling behavior of the black hole mass. The outermost gridpoint was chosen large enough to accommodate a range of the parameter p to good accuracy. The code was then run for several values of p in this range. For each value of p the code was run until a marginally outer trapped surface formed. The mass M of the black hole was then calculated. In figure 1 $\ln M$ is plotted as a function of $\ln |p - p^*|$.

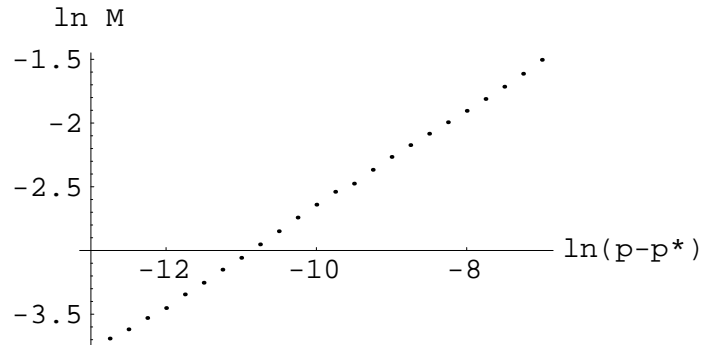


Figure 1

The points are well fit by a straight line whose slope is ≈ 0.38 . Thus the mass behaves like $M \propto (p - p^*)^\gamma$ where $\gamma \approx 0.38$. This is consistent with the results of references [1,5].

Next the code was run to treat the critical solution. The parameter p was set to p^* and the outermost gridpoint was set to its optimum value. Let u^* be the value of u at which the singularity forms. Define T and R by $T \equiv -\ln(u^* - u)$ and $R \equiv re^T$. Then the periodic self-similar property of the critical solution is that $h(R, T)$ is a periodic function of T .

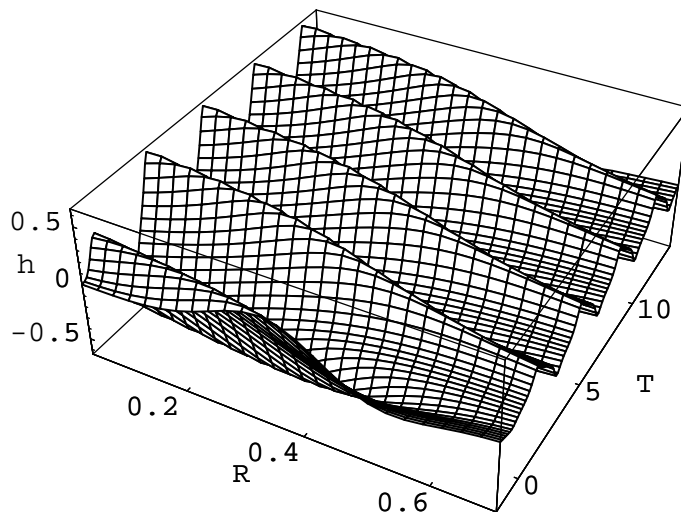


Figure 2

In figure 2 the quantity h is plotted as a function of R and T . After a certain amount of evolution the scalar field settles down to a behavior that seems to be periodic in T . To examine this apparent periodicity more carefully we pick an identifiable set of times: those times at which the maximum of h occurs at $r = 0$. The corresponding values of T are $T_1 \approx 2.58$, $T_2 \approx 6.02$, $T_3 \approx 9.47$ and $T_4 \approx 12.95$. Note that these times are equally spaced in T with a spacing $\Delta T = 3.45$ in agreement with the result found by Choptuik. We then plot $h(R)$ at each of these times to see whether this function is the same at each time.

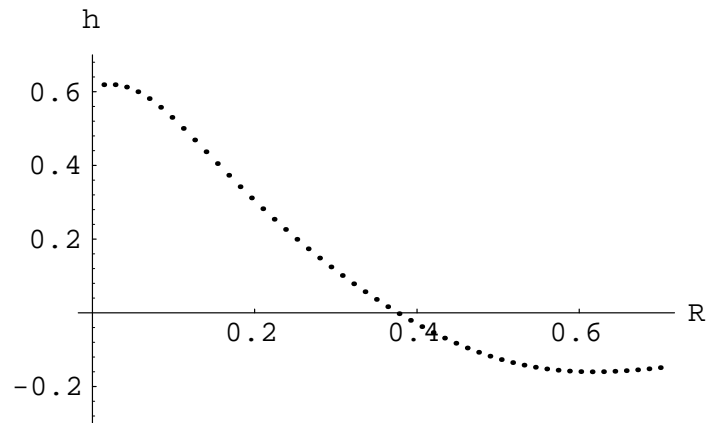


Figure 3

Figure 3 shows $h(R, T_1)$.

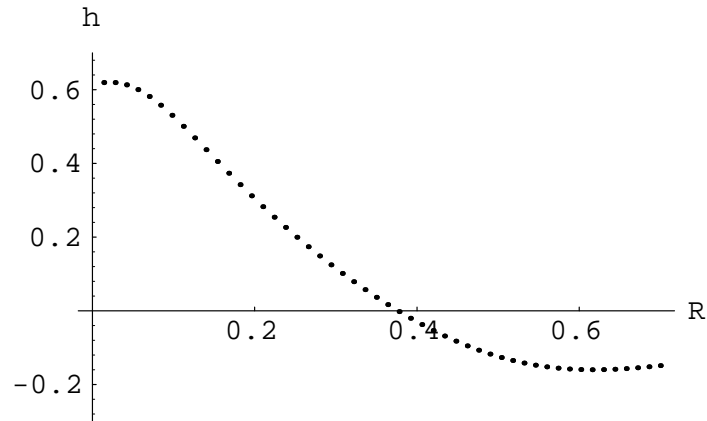


Figure 4

Figure 4 shows $h(R, T_1)$ and $h(R, T_2)$. Note that the functions agree. I emphasize that this figure has two *different* functions $h(R, T_1)$ and $h(R, T_2)$ plotted on the same graph. The agreement is so good that one cannot tell that the two functions differ.

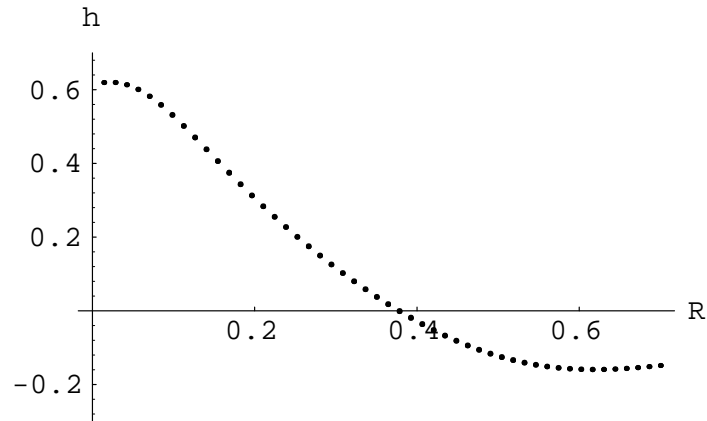


Figure 5

Figure 5 shows $h(R, T_1)$, $h(R, T_2)$ and $h(R, T_3)$ plotted together on the same graph. Again the agreement is so good that one cannot tell that the functions differ.

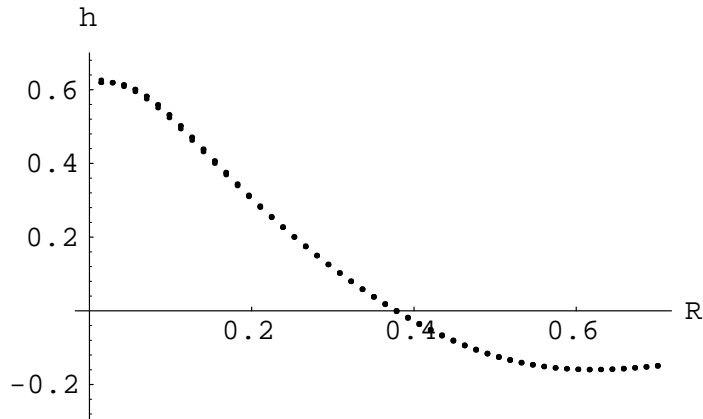


Figure 6

Figure 6 shows $h(R, T_1)$, $h(R, T_2)$, $h(R, T_3)$ and $h(R, T_4)$ plotted together on the same graph. Here the disagreement between the functions is barely visible.

Thus it is clear that after some initial evolution the scalar field of the critical solution settles down to an evolution that is periodic in T . Therefore we have confirmed, using a completely different algorithm from that of reference [1], that the critical solution spacetime has periodic self-similarity.

ACKNOWLEDGMENTS

It is a pleasure to thank Beverly Berger, Chuck Evans and G. Comer Duncan for helpful discussions. I thank the Institute for Theoretical Physics, University of California, Santa

Barbara, the Aspen Center for Physics and the Astronomy Department of the University of Michigan for hospitality. Computations were performed using the facilities of the National Center for Supercomputing Applications at The University of Illinois. This work was supported in part by National Science Foundation Grant PHY94-08439 and Research Corporation Grant C-3703 to Oakland University.

REFERENCES

- [1] M. Choptuik, Phys. Rev. Lett. **70**, 9 (1993)
- [2] A. Abrahams and C. Evans, Phys. Rev. Lett. **70**, 2980, (1993)
- [3] D. Christodoulou, Comun. Math. Phys. **105**, 337 (1986); D. Christodoulou, Comun. Math. Phys. **109**, 613 (1987)
- [4] D. Goldwirth and T. Piran, Phys. Rev. **D36**, 3575 (1987)
- [5] C. Grundlach, R. Price and J. Pullin, Phys. Rev. **D49**, 890 (1994)

FIGURES

FIG. 1. Scaling of the black hole mass. $\ln M$ is plotted vs. $\ln(p - p^*)$. The result is a straight line whose slope is the critical exponent $\gamma \approx 0.38$.

FIG. 2. Behavior of h as a function of the logarithmic coordinates R and T . After some initial evolution h is a periodic function of T . This demonstrates the periodic self-similarity of the spacetime.

FIG. 3. $h(R)$ is plotted at T_1

FIG. 4. $h(R)$ is plotted at two *different* times T_1 and T_2 on the *same* graph. Note that the two functions agree completely.

FIG. 5. $h(R)$ is plotted at three *different* times T_1, T_2 and T_3 on the *same* graph. Note that the three functions agree completely.

FIG. 6. $h(R)$ is plotted at four *different* times T_1, T_2, T_3 and T_4 on the *same* graph. One can barely see the disagreement among these functions.